PET Imaging of Prostate Cancer Xenografts with a Highly Specific Antibody against the Prostate-Specific Membrane Antigen

Ursula Elsässer-Beile[1], Gerald Reischl[2], Stefan Wiehr[3], Patrick Bühler[1], Philipp Wolf[1], Karen Alt[1,4], John Shively[5], Martin S. Judenhofer[3], Hans-Jürgen Machulla[2], and Bernd J. Pichler[3]

[1]Department of Urology, University of Freiburg, Freiburg, Germany; [2]Radiopharmacy, Department of Radiology, University of Tübingen, Tübingen, Germany; [3]Laboratory for Preclinical Imaging and Imaging Technology of the Werner Siemens-Foundation, Department of Radiology, University of Tübingen, Tübingen, Germany; [4]Faculty of Biology, University of Freiburg, Freiburg, Germany; and [5]Division of Immunology and Beckman Research Institute, City of Hope National Medical Center, Duarte, California

Prostate-specific membrane antigen (PSMA), a transmembrane glycoprotein, is highly expressed by virtually all prostate cancers and is currently the focus of several diagnostic and therapeutic strategies. We have previously reported on the generation of several monoclonal antibodies (mAb) and antibody fragments that recognize and bind with high affinity to the extracellular domain of cell-adherent PSMA. This article reports the in vivo behavior and tumor uptake of the radiolabeled anti-PSMA mAb 3/A12 and its potential as a tracer for PET. **Methods:** The mAb 3/A12 was conjugated with the chelating agent 1,4,7,10-tetraazacyclododecane-*N,N′,N″,N‴*-tetraacetic acid (DOTA) and radiolabeled with ^{64}Cu. Severe combined immunodeficient mice bearing PSMA-positive C4-2 prostate carcinoma xenografts were used for small-animal PET imaging. Mice with PSMA-negative DU 145 tumors served as controls. For PET studies, each animal received 20–30 μg of radiolabeled mAb corresponding to an activity of 7.6–11.5 MBq. Imaging was performed 3, 24, and 48 h after injection. After the last scan, the mice were sacrificed and tracer in vivo biodistribution was measured by γ-counting. **Results:** Binding of the mAb 3/A12 on PSMA-expressing C4-2 cells was only minimally influenced by DOTA conjugation. The labeling efficiency using ^{64}Cu and DOTA-3/A12 was 95.3% ± 0.3%. The specific activity after ^{64}Cu labeling was between 327 and 567 MBq/mg. After tracer injection, static small-animal PET images of mice with PSMA-positive tumors revealed a tumor-to-background ratio of 3.3 ± 1.3 at 3 h, 7.8 ± 1.4 at 24 h, and 9.6 ± 2.7 at 48 h. In contrast, no significant tracer uptake occurred in the PSMA-negative DU 145 tumors. These results were confirmed by direct counting of tissues after the final imaging. **Conclusion:** Because of the high and specific uptake of ^{64}Cu-labeled mAb 3/A12 in PSMA-positive tumors, this ligand represents an excellent candidate for prostate cancer imaging and potentially for radioimmunotherapy.

Key Words: prostate-specific membrane antigen; radioimmunoimaging; tumor localization; PET

J Nucl Med 2009; 50:606–611
DOI: 10.2967/jnumed.108.058487

Received Apr. 3, 2008; revision accepted Dec. 29, 2008.
For correspondence or reprints contact: Bernd J. Pichler, Laboratory for Preclinical Imaging and Imaging Technology of the Werner Siemens-Foundation, Department of Radiology, University of Tübingen, Röntgenweg, 13 72076 Tübingen, Germany.
E-mail: bernd.pichler@med.uni-tuebingen.de

Despite recent improvements in early detection and treatment, prostate cancer continues to be the most common malignancy and second leading cause of cancer-related mortality in men in the West.

The face of prostate cancer detection is changing. The widespread use of prostate-specific antigen screening has led to a dramatic downstaging of prostate cancer at diagnosis (*1*). The cancers detected today are smaller, of lower stage, and of lower grade than they were 20 y ago, but a wide range of aggressiveness remains.

Imaging has played a critical role in prostate cancer staging and in the detection of metastasis since the development of radiography of the axial skeleton. However, the precise indications for and specificity of imaging methods such as radionuclide bone scanning, CT, MRI or spectroscopy, ultrasonography, and combined PET/CT remain under debate (*2*). Clinical PET studies on prostate cancer have been performed with the non–tumor-specific glucose analog ^{18}F-FDG (*3*) or the ^{11}C-choline tracer for membrane synthesis (*4*).

As an alternative to PET tracers based on small molecules, radiolabeled antibodies that localize specifically to human malignancies are a new approach (*5*). Thus, antibodies or antibody fragments against antigens such as carcinoembryonic antigen (*6–8*), L1-CAM (*9*), or p185 (*10*) have been used for PET of various tumors, but not for prostate cancer.

Recent advances in expression profiling have identified several markers for prostate cancer. Of these, the prostate-specific membrane antigen (PSMA) has proved to be an excellent target because this 100-kDa type II transmembrane glycoprotein is highly expressed by virtually all prostate cancers (*11,12*). In contrast to other highly restricted prostate-related antigens, such as the prostate-specific antigen and prostatic acid phosphatase, which are secretory proteins, PSMA is an integral membrane protein and is not released into the circulation (*13*). PSMA expres-

sion is highly prostate-specific and has been shown to be upregulated in poorly differentiated and advanced prostate cancer (*14*). The PSMA protein is expressed as a homodimer with a compact 3-dimensional structure on the cell surface of prostate epithelial cells and exhibits an extensive extracellular domain of 707 amino acid (*15,16*). Antibodies or antibody fragments targeting this specific extracellular structure can bind to and can be internalized in PSMA-expressing cells (*17*).

Recently, we reported the development of 3 IgG monoclonal antibodies (mAbs) that react with cell-adherent PSMA and bind with high affinity to PSMA-expressing prostate cancer cells (*18*). The present study dealt with the in vivo behavior, biodistribution, and tumor uptake of one of these mAbs labeled with ^{64}Cu-1,4,7,10-tetraazacyclododecane-*N,N′,N″,N‴*-tetraacetic acid (DOTA).

MATERIALS AND METHODS

Cell Lines

The PSMA-positive, androgen-independent prostate cancer LNCaP subline C4-2 and the PSMA-negative prostate cancer cell line DU 145 were obtained from ATCC. Cells were propagated by serial passage in RPMI 1640 medium, supplemented with penicillin (100 U/mL), streptomycin (100 mg/L), and 10% fetal calf serum (Biochrom) at 37°C in a humidified atmosphere of 5% CO_2.

The Hybridoma 3/A12 mAb

Generation of the hybridoma 3/A12 mAb (IgG1, anti-PSMA) was described previously (*18*). In brief, SP2-0 myeloma cells were fused with spleen cells from a BALB/c mouse, immunized intraperitoneally 5 times with 200 μL of mammalian protein extraction reagent lysate from LNCaP cells in complete Freund's adjuvant.

The mAb was purified using a 1-mL HiTrap protein G affinity column according to the manufacturer's instructions (Amersham Biosciences).

Flow Cytometry

Target cells (C4-2 and DU 145) were freshly harvested from tissue culture flasks, and a single-cell suspension was prepared in phosphate-buffered saline (PBS) with 3% fetal calf serum and 0.1% NaN_3. Approximately 10^5 cells were incubated with 50 μL of primary mAb 3/A12 at concentrations between 0.15 and 2,600 nM for 1 h on ice. After 3 rounds of washing with PBS, the cells were incubated with 25 μL of phycoerythrin-labeled goat antimouse IgG (Becton Dickinson) for 40 min on ice. The cells were then washed repeatedly and resuspended in 200 μL of PBS containing 1 μg of propidium iodide per milliliter, 3% fetal calf serum, and 0.1% NaN_3. The relative fluorescence of stained cells was measured using a FACScan flow cytometer and the CellQuest software (Becton Dickinson). Mean fluorescence intensity values were considered after subtraction of the background staining with phycoerythrin-labeled goat antimouse IgG alone.

Preparation of DOTA-3/A12 mAb

An aliquot of 4 mg of mAb 3/A12 in 1 mL of PBS was dialyzed against 0.1 M Na_2HPO_4, pH 7.5, containing 1.2 g of Chelex 100 (Fluca) per liter, for 42 h at 4°C. Then, 80 μL of a freshly prepared 10 mg/mL solution of DOTA-mono (N-hydroxysuccinimide ester) (Macrocyclics) in 0.1 M Na_2HPO_4 were added. The reaction mixture was incubated at 4°C for 24 h with continuous end-over-end mixing, after which it was dialyzed against 10 mM Na_2HPO_4/150 mM NaCl, pH 7.5, containing 1.2 g of Chelex 100 per liter for 24 h at 4°C. The conjugate was then dialyzed against 0.25 M ammonium acetate, pH 7.0, containing 1.2 g of Chelex 100 per liter for 140 h at 4°C with 5 buffer changes.

Radiolabeling of DOTA-3/A12

^{64}Cu was produced in Tübingen at the PETtrace cyclotron (12.5 MeV; GE Healthcare) by irradiation of ^{64}Ni metal electroplated on a platinum/iridium plate (90/10) (20 mg, >98% enrichment; Isoflex) via the ^{64}Ni(p,n)^{64}Cu nuclear reaction and separated from ^{64}Ni and other metallic impurities after dissolution using ion exchange chromatography (*19*). Radiolabeling was performed according to a modified procedure described in the literature (*20*). Briefly, 100 μL of a solution of the DOTA-conjugated antibody in a 1.5-mL Eppendorf cap (4.3 mg/mL in 0.25 M NH_4OAc, pH 7.0) were incubated with approximately 100 μL of ^{64}Cu (180–280 MBq) in 0.01 M HCl at 40°C for 40 min. pH was checked to be 5.5. Afterward, 20 μL of 10 mM diethylenetriaminepentaacetic acid and 100 μL of 1% bovine serum albumin were added. Quality control was performed using thin-layer chromatography (silica gel 60, F_{254}; Merck) and high-performance liquid chromatography (BioSil SEC 125-5 [Bio-Rad]; 300 × 7.8 mm; PBS; 1 mL/min; 220 nm).

SCID Mouse Xenograft Model

Six-week-old male severe combined immunodeficient (SCID) mice were purchased from Charles River Laboratories. The animals were kept under sterile and standardized environmental conditions (20°C ± 1°C room temperature, 50% ± 10% relative humidity, 12-h light–dark rhythm) and received autoclaved food, water, and bedding. All experiments were performed according to the German Animal Protection Law with permission from the responsible local authorities. For tumor inoculation, 2×10^6 C4-2 cells or 2×10^6 DU 145 cells in 100 μL of PBS were mixed with 100 μL of Matrigel (Collaborative Biomedical Products) at 4°C and administered subcutaneously in the right flank of each animal. Growing tumors were palpated, and the diameters were measured by a caliper rule and recorded 3 times a week.

PET Studies and Biodistribution

For the PET experiment, tumor mice were imaged using an Inveon dedicated small-animal PET scanner (Siemens Preclinical Solutions), yielding a spatial resolution of about 1.3 mm in the reconstructed image. The awake animals were lightly restrained and injected with 20–30 μg of ^{64}Cu-DOTA-3/A12 mAb via a lateral tail vein. A 10-min static PET scan was obtained 3, 24, and 48 h after tracer injection. During imaging, the animals were anesthetized with a mixture of 1.5% isoflurane and 100% oxygen. The animals were centered in the field of view of the PET scanner. Anesthesia was monitored by measuring respiratory frequency, and the body temperature was kept at 37°C by a heating pad underneath the animal. PET data were acquired in list mode, graphed in one 10-min time frame, and reconstructed using an iterative ordered-subset expectation maximization algorithm. Image files were analyzed using AsiPro software (Siemens Preclinical Solutions).

After the last PET scan, the animals were sacrificed by cervical dislocation under deep anesthesia and dissected. Tumors and organs were removed and measured together with an aliquot of

injected solution in the γ-counter (Wizard single-detector γ-counter; Perkin Elmer) using an energy window of between 425 and 640 keV. Results are expressed as percentage injected dose (%ID) per gram of tissue.

Statistical Analysis

All quantitative data are reported as mean ± 1 SD. Statistical analysis was performed using a 2-tailed *t* test; data were considered as statistically significant for *P* values of 0.05 or less.

RESULTS

Binding of DOTA-Labeled 3/A12 mAb to C4-2 Cells

Flow cytometry showed that the mAb 3/A12 strongly stained PSMA-expressing C4-2 cells whereas PSMA-negative DU 145 cells were not affected. At antigen saturation concentrations, the corrected mean fluorescence intensity was about 500, with a percentage of positive cells ranging from 96% to 98%.

The binding properties of 3/A12 mAb and DOTA-conjugated 3/A12 were compared by treating C4-2 cells with increasing concentrations (between 0.15 and 2,600 nM) of the primary mAb (3/A12 and DOTA-3/A12) followed by incubation with a saturating amount of phycoerythrin-labeled goat antimouse IgG followed by cytofluorometric analysis. The concentration reaching a 50% saturation of PSMA sites was 10 nM for 3/A12 and 15 nM for DOTA-3/A12, indicating only a minimal reduction of the binding capacity after derivatization (Fig. 1). When Cu-DOTA-3/A12 (labeled with nonradioactive copper) was measured in a similar way, no alteration of the immunoreactivity was found.

Serum Stability of DOTA-3/A12 mAb

The DOTA-conjugated mAb 3/A12 and the nonconjugated antibody were incubated in PBS with 20% SCID mouse serum for 24 h at 37°C. Then, the binding to C4-2 cells was measured by flow cytometry at concentrations of 0.15–800 nM. After serum incubation, the concentration reaching a 50% saturation of PSMA sites on C4-2 cells shifted from 10 to 15 nM for 3/A12 and from 15 to 18 nM for DOTA-3/A12, showing only a minimal reduction of the immunoreactivity (Fig. 1).

Additionally, we incubated ^{64}Cu-DOTA 3/A12 for 3, 24, and 48 h in PBS and 20% SCID mouse serum at 37°C and measured the purity (stability) by thin-layer chromatography. At these time points, the radiochemical purity decreased from 94% (without incubation) to 93% (3 h, PBS/serum), 89.6% (24 h, PBS), 92% (24 h, serum), 90% (48 h, PBS), and 63% (48 h, serum).

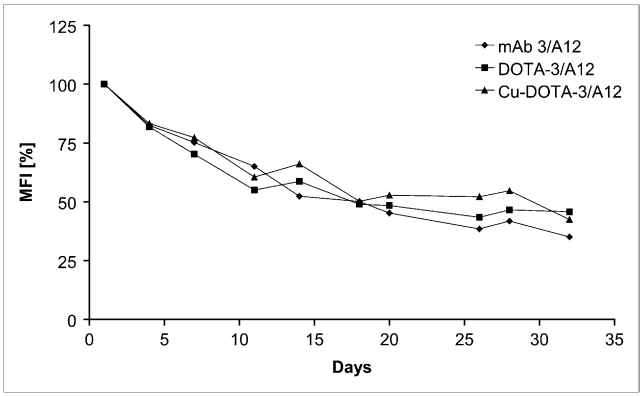

FIGURE 1. Binding of 3/A12 mAb and DOTA-3/A12 mAb, with and without serum preincubation, to PSMA-positive C4-2 cells. Cells were treated with increasing concentrations (0.15–800 nM) of first-step anti-PSMA mAb followed by incubation with saturating amount of second-step phycoerythrin-labeled goat antimouse IgG followed by cytofluorometric analysis. MFI = mean fluorescence intensity.

Blood Immunoreactivity of Unconjugated and Functionalized 3/A12 mAb

For measuring immunoreactivity and clearance in SCID mice, 3/A12 mAb, DOTA-3/A12, and DOTA-3/A12 labeled with nonradioactive copper were each injected into 3 mice at a single dose of 25 μg. Blood was collected at different time points between 1 and 32 d after mAb injection. Then, the immunoreactivity was determined by flow cytometry. As shown in Figure 2, the serum activity of 3/A12, DOTA-3/A12, and Cu-DOTA-3/A12 decreased slowly. From the curves, a serum half-life of about 18 d for 3/A12, DOTA-3/A12, and Cu-DOTA-3/A12 was estimated.

Tumor Inoculation

In the described SCID mouse model, in about 90% of the animals xenotransplanted with C4-2 or DU 145 cells, solid tumors developed within 14 d after inoculation. Imaging experiments were performed when tumors had reached a diameter of about 4 mm, corresponding to a volume of about 30–50 mm^3.

PET

The radiochemical purity after labeling DOTA-3/A12 with ^{64}Cu was 95.3% ± 0.3%. The specific activity was

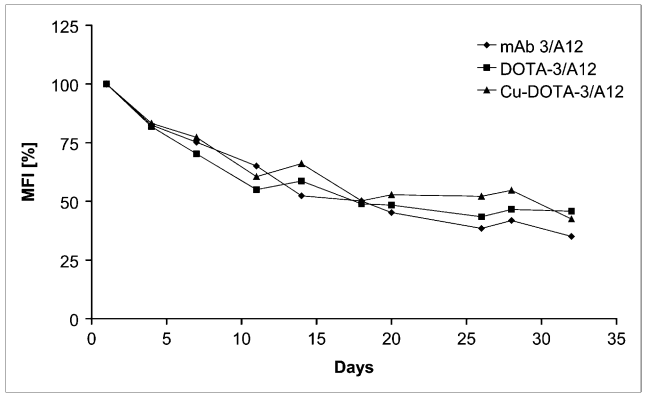

FIGURE 2. Blood immunoreactivity of 3/A12, DOTA-3/A12, and copper-DOTA-3/A12 in SCID mice after intravenous injection of 25 μg of mAb. Serum levels are given as mean fluorescence intensity (MFI) measured by flow cytometry.

between 327 and 567 MBq/mg, with a mean of 442 ± 120 MBq/mg in 3 independent labeling procedures.

Each animal (n = 8) received between 20 and 30 μg of radiolabeled mAb, corresponding to an activity of 7.6–11.5 MBq.

Although the blood activity of the mAb was rather high, static small-animal PET images of mice bearing PSMA-positive tumors revealed a tumor-to-muscle ratio of 3.3 ± 1.3 at 3 h, 7.8 ± 1.4 at 24 h, and 9.6 ± 2.7 at 48 h after tracer injection (Fig. 3, positive control). In sharp contrast, the PSMA-negative DU 145 tumors showed only faint tracer uptake at any measured time point (Fig. 3, negative control). The difference between DU 145 and C4-2 tumors was highly significant at 24 and 48 h after injection of the radiolabeled mAb ($P < 0.001$).

The binding of ^{64}Cu-DOTA-3/A12 mAb was successively blocked by injecting mice with 250, 500, and 700 μg of nonradioactive 3/A12 mAb 3 h before radiotracer injection (Figs. 3 and 4).

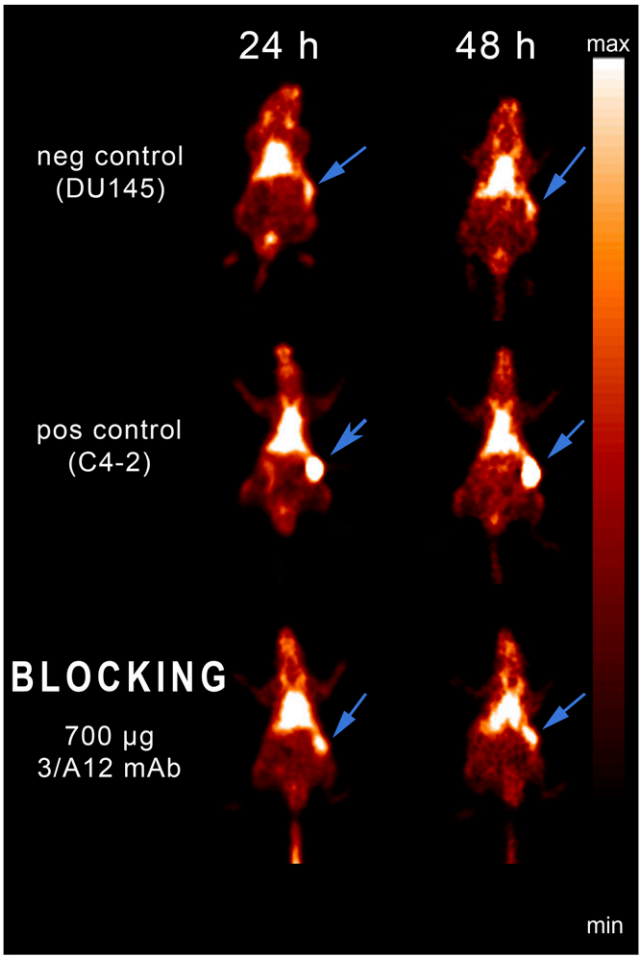

FIGURE 3. Small-animal PET imaging of mice bearing PSMA-positive C4-2 tumors (pos control, C4-2) and PSMA-negative DU 145 tumors (neg control, DU145) 24 and 48 h after injection of ^{64}Cu-DOTA-3/A12 mAb. Blocking experiments were performed by injecting unlabeled 3/A12 mAb 3 h before injection of ^{64}Cu-labeled mAb (blocking, 700 μg of 3/A12 mAb). Arrows indicate position of tumors.

Tracer Biodistribution

The in vivo biodistribution of ^{64}Cu-DOTA–radiolabeled mAb 3/A12 was quantitatively assessed by γ-counting of selected isolated organs from mice bearing PSMA-positive C4-2 tumors (n = 8) and from animals with DU 145 tumors (n = 7) 48 h after tracer application (Fig. 5). These data revealed a significantly higher uptake of 35.1 ± 8.0 %ID/g in C4-2 tumors, compared with 12.8 ± 2.7 %ID/g in DU 145 tumors ($P < 0.001$). The activity remaining in the blood was 16.2 ± 9.5 %ID/g in mice with C4-2 tumors and 17.9 ± 1.8 %ID/g in mice with DU 145 tumors. Figure 5 shows the mean tracer uptake 48 h after injection in the tumor and blood and in addition in muscle (1.3 ± 0.3 %ID/g), heart (5.1 ± 1.0 %ID/g), stomach (2.1 ± 0.4 %ID/g), kidney (5.5 ± 0.6 %ID/g), and colon (2.6 ± 0.4 %ID/g). Measured %ID differed by approximately a factor of 2 between the postmortem biodistribution data and in vivo PET data. This difference, a lower %ID/cm^3 in PET data than in the postmortem biodistribution by γ-counting, is caused mainly by non–attenuation-corrected animal PET data and partial-volume effects. However, the ratios in PET and γ-counting between PSMA-positive and DU 145 tumors were comparable.

DISCUSSION

On the basis of in vitro studies, we previously reported that mAbs specific to the external domain of native cell–adherent PSMA are excellent agents for targeting viable PSMA-positive tumors (*18*). The aim of the present study was to test if one of these mAbs may be suitable for PET of prostate cancer.

The tracer was based on the anti-PSMA mAb 3/A12. Radiolabeling with ^{64}Cu through a DOTA moiety conju-

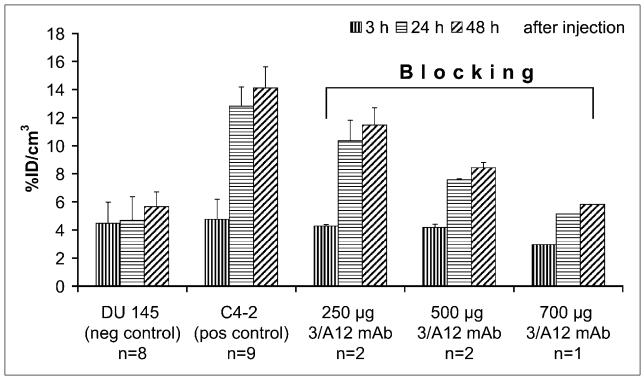

FIGURE 4. Blocking of ^{64}Cu-DOTA-3/A12 mAb uptake in C4-2 tumors with 250, 500, or 700 μg of nonradioactive 3/A12 mAb, given 3 h before radiotracer injection. %ID/cm^3 from mice bearing DU 145 tumors (negative control) or C4-2 tumors (positive control) 3, 24, and 48 h after injection of ^{64}Cu-DOTA-3/A12 are shown.

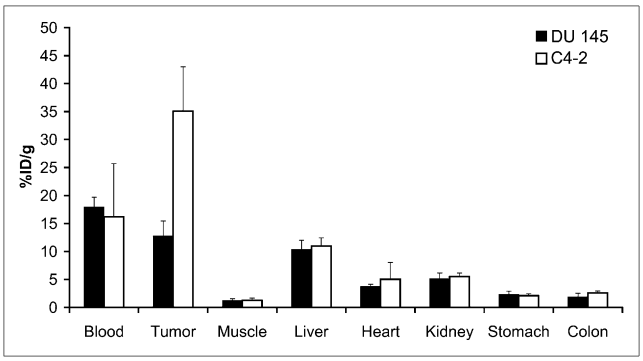

FIGURE 5. Biodistribution by γ-counting of ^{64}Cu-DOTA-3/A12 in various organs of mice 48 h after injection.

gated to the mAb was accomplished without loss of immunoreactivity. Small-animal PET imaging studies showed that the ^{64}Cu-labeled mAb 3/A12 bound specifically to C4-2 tumors, whereas tracer uptake in PSMA-negative DU 145 tumors remained at the background level. This comparison with the PSMA-negative control tumor supports antigen binding as the major mechanism of localization. Sufficient tumor-to-background uptake ratios in PSMA-positive tumors were already reached 3 h after tracer injection. Target-to-background ratios and the resultant quality of the images improved when the imaging time was extended to 24 and 48 h after injection. The specificity of the radiolabeled mAb 3/A12 to PSMA was proven by the blocking experiments, in which a nearly full receptor blockade could be reached with 700 μg of nonradiolabeled mAb. The time of application of the unlabeled mAb was 3 h before tracer injection. This time was chosen according to our own unpublished internalization data. The γ-counting results showed a high tracer concentration in the blood over 48 h. This result was expected for mAb in vivo imaging (*21*). However, this high blood concentration was compensated for by a specific binding of the radiolabeled mAb, leading to a tumor-to-background ratio that was sufficient for PET. The 12.7-h half-life of ^{64}Cu allows for a mAb-labeling and animal-handling timing schedule that is convenient and will be acceptable, in terms of radiation safety, for potential future clinical applications. Such a schedule would be especially acceptable in view of the low levels at which ^{64}Cu uptake remained in other organs, such as kidney, muscle, or liver.

Copper–DOTA complexes are not stable in vivo, and ^{64}Cu may be transchelated to other proteins (*22*). Also, ^{64}Cu-DOTA 3/A12 has been shown to be unstable on incubation with SCID mouse serum for 48 h in vitro, and this instability may also be expected in vivo. On the other hand, we have demonstrated that PSMA is rapidly internalized into PSMA-expressing cells after binding of the anti-PSMA mAb 3/A12 (*18*), and conjugates of 3/A12 are also internalized rapidly. This internalization of the radiometal-labeled antibody is suggested to result in metabolism and trapping of the radioactivity at the tumor site, maintaining the signal (*21*).

The use of PSMA as an in vivo target has been initially validated by immunoscintigraphy trials with the mAb 7E11/CYT-356 (capromab pendetide [ProstaScint]; Cytogen Corp.) (*23–26*). However, this mAb targets an intracellular portion of the PSMA molecule and therefore can target only necrotic or apoptotic cells (*27*). This fact is thought to be the basis of its ability to target soft-tissue sites but not bone metastases (*28*).

A major advantage has been the development of a series of mAbs that bind to the extracellular portion of PSMA (*29*). These antibodies have been shown to bind to viable prostate epithelial cells with high affinity (*30*). One of these, J591, has been extensively studied in preclinical models, in which it showed a high tumor-to-nontumor organ ratio in nude mice bearing LNCaP tumors (*31,32*). These studies were followed by several clinical trials using J591 labeled with different nuclides for radioimmunoscintigraphy and radioimmunotherapy (*33*). However, to our knowledge, no PET study with J591 or other anti-PSMA mAbs has been published.

We are aware that imaging with a mAb bears the problem of a prolonged biologic half-life of the intact antibody with a slow blood clearance. For further development toward a clinical application, smaller antibody fragments may have a better relationship between tumor uptake and blood clearance (*21*). Therefore, Fab and $(Fab)_2$ antigen-binding fragments of the mAb 3/A12, as well as a recombinant antibody fragment and diabody, are currently under investigation.

CONCLUSION

The present study demonstrated that the PSMA-specific mAb 3/A12 directed against the native cell–adherent molecule may be an ideal tool for the development of novel PET tracers for prostate cancer imaging. For clinical applications, the development of recombinant humanized antibody fragments from 3/A12 is presently under investigation.

REFERENCES

1. Jemal A, Siegel R, Ward E, et al. Cancer statistics, 2006. *CA Cancer J Clin.* 2006;56:106–130.
2. Eschmann SM, Pfannenberg AC, Rieger A, et al. Comparison of ^{11}C-choline-PET/CT and whole body-MRI for staging of prostate cancer. *Nuklearmedizin.* 2007;46:161–168.
3. Oyama N, Akino H, Suzuki Y, et al. Prognostic value of 2-deoxy-2-[F-18]fluoro-D-glucose positron emission tomography imaging for patients with prostate cancer. *Mol Imaging Biol.* 2002;4:99–104.
4. Lawrentschuk N, Davis ID, Bolton DM, Scott AM. Positron emission tomography and molecular imaging of the prostate: an update. *BJU Int.* 2006;97:923–931.
5. Moffat FL Jr, Gulec SA, Serafini AN, et al. A thousand points of light or just dim bulbs? Radiolabeled antibodies and colorectal cancer imaging. *Cancer Invest.* 1999;17:322–334.
6. Wu AM, Yazaki PJ, Tsai S, et al. High-resolution microPET imaging of carcinoembryonic antigen-positive xenografts by using a copper-64-labeled engineered antibody fragment. *Proc Natl Acad Sci USA.* 2000;97:8495–8500.

7. Sundaresan G, Yazaki PJ, Shively JE, et al. ^{124}I-labeled engineered anti-CEA minibodies and diabodies allow high-contrast, antigen-specific small-animal PET imaging of xenografts in athymic mice. *J Nucl Med.* 2003;44:1962–1969.
8. Kenanova V, Olafsen T, Crow DM, et al. Tailoring the pharmacokinetics and positron emission tomography imaging properties of anti-carcinoembryonic antigen single-chain Fv-Fc antibody fragments. *Cancer Res.* 2005;65:622–631.
9. Zimmermann K, Grunberg J, Honer M, Ametamey S, Schubiger PA, Novak-Hofer I. Targeting of renal carcinoma with $^{67/64}$Cu-labeled anti-L1-CAM antibody chCE7: selection of copper ligands and PET imaging. *Nucl Med Biol.* 2003;30:417–427.
10. Olafsen T, Kenanova VE, Sundaresan G, et al. Optimizing radiolabeled engineered anti-p185HER2 antibody fragments for in vivo imaging. *Cancer Res.* 2005;65:5907–5916.
11. Ghosh A, Heston WD. Tumor target prostate specific membrane antigen (PSMA) and its regulation in prostate cancer. *J Cell Biochem.* 2004;91:528–539.
12. Sweat SD, Pacelli A, Murphy GP, Bostwick DG. Prostate-specific membrane antigen expression is greatest in prostate adenocarcinoma and lymph node metastases. *Urology.* 1998;52:637–640.
13. Troyer JK, Beckett ML, Wright GL Jr. Detection and characterization of the prostate-specific membrane antigen (PSMA) in tissue extracts and body fluids. *Int J Cancer.* 1995;62:552–558.
14. Murphy GP, Elgamal AA, Su SL, Bostwick DG, Holmes EH. Current evaluation of the tissue localization and diagnostic utility of prostate specific membrane antigen. *Cancer.* 1998;83:2259–2269.
15. Davis MI, Bennett MJ, Thomas LM, Bjorkman PJ. Crystal structure of prostate-specific membrane antigen, a tumor marker and peptidase. *Proc Natl Acad Sci USA.* 2005;102:5981–5986.
16. Mesters JR, Barinka C, Li W, et al. Structure of glutamate carboxypeptidase II, a drug target in neuronal damage and prostate cancer. *EMBO J.* 2006;25:1375–1384.
17. Schulke N, Varlamova OA, Donovan GP, et al. The homodimer of prostate-specific membrane antigen is a functional target for cancer therapy. *Proc Natl Acad Sci USA.* 2003;100:12590–12595.
18. Elsässer-Beile U, Wolf P, Gierschner D, Bühler P, Schultze-Seemann W, Wetterauer U. A new generation of monoclonal and recombinant antibodies against cell-adherent prostate specific membrane antigen for diagnostic and therapeutic targeting of prostate cancer. *Prostate.* 2006;66:1359–1370.
19. McCarthy DW, Shefer RE, Klinkowstein RE, et al. Efficient production of high specific activity ^{64}Cu using a biomedical cyclotron. *Nucl Med Biol.* 1997;24: 35–43.
20. Lewis MR, Wang M, Axworthy DB, et al. In vivo evaluation of pretargeted ^{64}Cu for tumor imaging and therapy. *J Nucl Med.* 2003;44:1284–1292.
21. Wu AM, Senter PD. Arming antibodies: prospects and challenges for immunoconjugates. *Nat Biotechnol.* 2005;23:1137–1146.
22. Boswell CA, Sun X, Niu W, et al. Comparative in vivo stability of copper-64-labeled cross-bridged and conventional tetraazamacrocyclic complexes. *J Med Chem.* 2004;47:1465–1474.
23. Kahn D, Williams RD, Seldin DW, et al. Radioimmunoscintigraphy with 111indium labeled CYT-356 for the detection of occult prostate cancer recurrence. *J Urol.* 1994;152:1490–1495.
24. Sodee DB, Conant R, Chalfant M, et al. Preliminary imaging results using In-111 labeled CYT-356 (Prostascint) in the detection of recurrent prostate cancer. *Clin Nucl Med.* 1996;21:759–767.
25. Haseman MK, Reed NL, Rosenthal SA. Monoclonal antibody imaging of occult prostate cancer in patients with elevated prostate-specific antigen: positron emission tomography and biopsy correlation. *Clin Nucl Med.* 1996;21:704–713.
26. Seltzer MA, Barbaric Z, Belldegrun A, et al. Comparison of helical computerized tomography, positron emission tomography and monoclonal antibody scans for evaluation of lymph node metastases in patients with prostate specific antigen relapse after treatment for localized prostate cancer. *J Urol.* 1999;162: 1322–1328.
27. Troyer JK, Beckett ML, Wright GL Jr. Location of prostate-specific membrane antigen in the LNCaP prostate carcinoma cell line. *Prostate.* 1997;30:232–242.
28. Bander NH, Nanus DM, Milowsky MI, Kostakoglu L, Vallabahajosula S, Goldsmith SJ. Targeted systemic therapy of prostate cancer with a monoclonal antibody to prostate-specific membrane antigen. *Semin Oncol.* 2003;30:667–676.
29. Liu H, Moy P, Kim S, et al. Monoclonal antibodies to the extracellular domain of prostate-specific membrane antigen also react with tumor vascular endothelium. *Cancer Res.* 1997;57:3629–3634.
30. Smith-Jones PM, Vallabahajosula S, Goldsmith SJ, et al. In vitro characterization of radiolabeled monoclonal antibodies specific for the extracellular domain of prostate-specific membrane antigen. *Cancer Res.* 2000;60:5237–5243.
31. McDevitt MR, Barendswaard E, Ma D, et al. An alpha-particle emitting antibody ([^{213}Bi]J591) for radioimmunotherapy of prostate cancer. *Cancer Res.* 2000;60: 6095–6100.
32. Smith-Jones PM, Vallabhajosula S, Navarro V, Bastidas D, Goldsmith SJ, Bander NH. Radiolabeled monoclonal antibodies specific to the extracellular domain of prostate-specific membrane antigen: preclinical studies in nude mice bearing LNCaP human prostate tumor. *J Nucl Med.* 2003;44:610–617.
33. Olson WC, Heston WD, Rajasekaran AK. Clinical trials of cancer therapies targeting prostate-specific membrane antigen. *Rev Recent Clin Trials.* 2007;2: 182–190.